Detailed description of the research program

A Scientific background

The atmospheric jet stream is a fast stream of air, concentrated at subtropical or middle latitudes approximately 10 kilometers above the ground. It is tightly coupled to surface weather systems, through mutual interactions. The jet stream properties vary on a wide range of time scales, from days to years and even decades. Understanding the dynamical processes that control the jet variability is crucial for understanding climate variability in the subtropics and midlatitudes.

The response of the jet to climate change induced by the anthropogenic increase in greenhouse gas concentration is complex and is only partially understood (Shaw, 2019). The most prominent response detected in climate model simulations and in observations is a poleward shift of the jet (Woollings et al., 2023). The poleward jet shift is explained by dynamical mechanisms that do not depend on longitude, i.e. zonally symmetric mechanisms. However, the structure of the jet is zonally asymmetric and can be viewed as a combination of jets at certain large longitudinal sectors, covering the large oceanic basins and continents. The jet variability and response to climate change are often explained by applying zonally-symmetric arguments while referring to jets at certain longitudinal sectors. In this proposed research, we aim to investigate the extent to which jet dynamics across large longitudinal sectors are influenced by either zonally symmetric or asymmetric processes.

The jet is driven by two main mechanisms. **One mechanism** is conservation of absolute (planetary plus relative) angular momentum: Planetary angular momentum is highest at the equator and decreases toward the poles. Air rises at the tropics due to strong convection and moves poleward from the tropics in the upper branch of the Hadley circulation cell. The poleward moving air advects absolute angular momentum, increasing the relative angular momentum, proportional to the zonal wind (Held and Hou, 1980). This mechanism creates a strong jet at the subtropical edge of the Hadley cell in the upper troposphere, called a subtropical or thermally-driven jet (Lee and Kim, 2003). **Another mechanism** involves momentum transport by extratropical eddies, also called storms or weather systems. Due to potential vorticity conservation, extratropical eddies transfer zonal momentum into the latitude from which they propagate meridionally. As a result, they create a jet at midlatitudes, called a midlatitude, polar-front or eddy-driven jet (Lee and Kim, 2003). The conceptual distinction between the subtropical and eddy-driven jets is useful, but can be misleading, since the jet is generally affected by both mechanisms (Lachmy and Harnik, 2014, 2016), as well as by other processes, such as vertical advection of zonal momentum and diabatic processes that modify the potential vorticity. When considering the jet at a limited longitudinal sector these processes include also zonal advection of momentum, acceleration due to the pressure gradient force and Rossby wave propagation.

In this proposed research we wish to examine the processes that affect the jet at large longitudinal sectors. The jets are usually classified as subtropical or eddy-driven according to their characteristics. Theoretical arguments suggest that angular momentum advection drives a jet at the subtropical edge of the Hadley cell in the upper troposphere, while eddy momentum flux drives a jet inside the Ferrel cell (the midlatitude atmospheric

overturning circulation cell) with surface westerlies below the upper tropospheric jet. Following these considerations, the subtropical and eddy-driven jet latitudes are often defined as the latitudes of maximum vertical shear of the zonal wind, and maximum surface westerlies, respectively (e.g., Waugh et al., 2018). For example, during Southern Hemisphere (SH) winter, in the Indo-Pacific sector there is a strong persistent jet concentrated in the subtropical upper troposphere (Figure 1a) with weak lower tropospheric westerly winds below (Figure 1c), which is identified as a subtropical jet. In contrast, the jet in the Atlantic sector, during the same season, is concentrated at midlatitudes, accompanied by strong surface westerly winds, and tends to fluctuate in latitude, as characteristic of an eddy-driven jet. Similarly, the SH summer jet (Figure 1b,d) is classified as an eddy-driven jet (Kim and Lee, 2004). However, observational studies indicate that the driving mechanisms of the jet in each sector and season are a mixture of several processes (Williams et al., 2007; Li and Wettstein, 2012; Gillett et al., 2021; Spensberger et al., 2023).

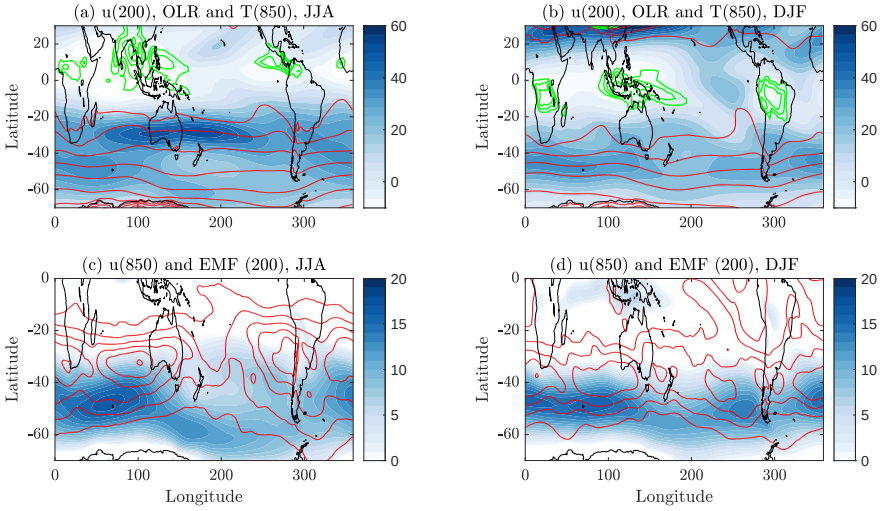

Figure 1: Zonal wind climatology (blue shading, in m s^{-1}), in the upper (200 hPa) (a,b) and lower (850 hPa) (c,d) troposphere , during Southern Hemisphere winter (June-August, JJA) (a,c) and summer (December-February, DJF) (b,d). The red contours in (a,b) represent the temperature at the 850 hPa pressure level, with a contour interval of 5 K, and the hottest contour level of 285 K. The red contours in (c,d) represent the eddy poleward momentum flux, where eddies are defined as deviations from the monthly mean, with a contour interval of 20 m^2 s^{-2}, starting from zero. The green contours in (a,b) show the outgoing longwave radiation (OLR), with a contour interval of 10 W m^2, from 180 to 220 W m^2. These contour levels represent the lowest values of OLR, which indicate strong convection.

The jet stream is affected by a combination of mechanisms, which play different roles at different longitudinal sectors. The sources of this zonal asymmetry vary between the two hemispheres. In the Northern Hemisphere (NH), continents and ocean currents play a major role in shaping the longitudinal structure of the jet (Nakamura et al., 2004), in addition to the effect of zonal asymmetries in tropical convection (Li and Wettstein, 2012; Hoskins and Yang, 2021). The SH jet flows mostly above the ocean, and its asymmetry is driven mainly by tropical convection that drives a localized Hadley circulation (Inatsu and Hoskins, 2004; Hoskins et al., 2020; Patterson et al., 2020) (tropical convection is indicated by the outgoing longwave radiation

(OLR) in Figure 1a). While the subtropical SH winter jet is driven by tropical convection, it is also affected by eddy momentum flux and Rossby wave propagation (Williams et al., 2007; Gillett et al., 2021; Hoskins et al., 2020; Hoskins and Yang, 2023). The eddy-driven jet in the SH winter has a zonally-asymmetric structure which is affected by the subtropical jet structure (Nakamura and Shimpo, 2004), Antarctic orography (Patterson et al., 2020) and Rossby wave propagation from the tropics (Ding et al., 2012).

Identifying the drivers of the jet structure and its variability is particularly challenging due to internal feedback mechanisms within the atmospheric circulation (Lorenz and Hartmann, 2001, 2003). The jet and the extratropical eddies are strongly coupled, therefore they cannot be considered as two separate components of the flow, with one being the driver of the other. While the interaction between the jet and the midlatitude eddies is responsible for much of the jet variability on daily to monthly time scales, the variability of the jet at longer time scales is affected by other processes, such as sea surface temperature (SST) variability, large-scale variability of the tropical convection, and coupled oceanic-atmospheric oscillations such as El-Niño Southern Oscillation (ENSO) (Liu et al., 2021). Our purpose here is to identify jet variability drivers at time scales ranging from monthly to interannual, and to quantify their relative roles in causing changes in the jet properties.

Causal relations cannot be strictly concluded from observational data, since specific processes cannot be isolated from other processes. Lagged correlations are often used to detect relations between different variables. If a significant correlation is found between one variable and another variable lagging it, this supports the hypothesis that the first variable drives the anomaly in the other variable, yet it does not prove causality. In recent years, more sophisticated statistical analysis methods were implemented in climate science, which enable a more rigorous detection of causal relations between variables (e.g., Kretschmer et al., 2016; Runge et al., 2019; Barnes et al., 2019; Kretschmer et al., 2021). These causal detection methods correct for the spurious effects of autocorrelation on the lagged correlation between two variables (Runge et al., 2014) and of confounding and mediating variables, assuming these variables are included in the analysis (Runge et al., 2019). We plan to apply causal detection methods to observational data of the jet properties and their potential drivers. This will allow us to obtain a quantitative estimation for the role of different jet driving processes at each longitudinal sector and season.

The response of the jet to climate change, as simulated by climate models, is affected by the historical circulation produced in each model. Biases in the representation of the longitudinal structure of the jet could lead to biases in the projected jet response. For example, the poleward shift of the eddy-driven jet has a large inter-model spread and is correlated with the historical jet latitude during SH winter (Curtis et al., 2020; Simpson et al., 2021), but this correlation is limited to the Pacific sector (Breul et al., 2023). Recent studies emphasize the role of tropical SST biases in driving zonally-asymmetric jet biases in climate models (Oudar et al., 2020; Waugh et al., 2020; Liu et al., 2021; Liu and Grise, 2023). We suggest combining analysis of climate model output data with causal detection methods to help identify and quantify biases in the representation of jet driving processes across large longitudinal sectors.

A direct way to examine jet driving processes is to perform controlled experiments using idealized numer-

ical global circulation models. We suggest to use an idealized moist aqua-planet model, and set it up with a localized tropical heating. The localized heating drives a localized Hadley cell and subtropical jet, similar to that observed in the atmosphere (see Figure 4 below). Our purpose is to isolate the effect of asymmetric tropical heating, which plays a dominant role in driving longitudinal transitions between jets of subtropical or eddy-driven characteristics (Inatsu and Hoskins, 2004; Patterson et al., 2020; Hoskins and Yang, 2023).

B Research objectives & expected significance

The overall goal of the proposed study is to advance the understanding of jet dynamics across large longitudinal sectors, where the jet properties are relatively uniform. The study will address the following questions:

1. To what extent can the climatology, variability and climate change response of the jet across large longitudinal sectors be explained using theoretical arguments that apply to a statistically zonally symmetric circulation?

2. What are the relative roles of different jet variability drivers over large longitudinal sectors in the two hemispheres, during different seasons? These drivers include angular momentum advection from the tropics, extratropical eddy activity generated due to an SST front, Rossby wave propagation from the tropics and stratospheric polar vortex variability.

3. What are the biases associated with jet driving mechanisms over large longitudinal sectors in climate models, and how are they related to projections of the jet response to climate change?

4. How does the jet respond to localized tropical heating, and what are the mechanisms controlling its longitudinally-dependent properties?

The current theoretical models are mostly applicable to zonally-symmetric conditions, while the actual jet is zonally-asymmetric. It has not yet been assessed if the dynamics of the jet over large longitudinal sectors are similar to those of a zonally-symmetric jet. Previous studies have used linear regression and lagged correlation methods to connect the jet variability to various climatic variables. While these methods add insight to the processes leading to jet variability, they do not imply causal relations, and thus are not sufficient for concluding which dynamical mechanisms are more important. The proposed research will use novel causal detection methods, that correct for various spurious effects and enable a more rigorous analysis of causal relations between variables. By combining these statistical analyses of observational and climate model data with controlled numerical experiments using an idealized model, we will be able to isolate the processes leading to the observed jet structure and variability. This study is expected to contribute to a better understanding of the jet response to external forcing related to interannual variability and anthropogenic climate change. This improved understanding could help interpret climate model projections in a more knowledgable way, thus reducing the uncertainty in future jet dynamics.

C Detailed description of the proposed work

C.1 Working hypothesis

The main hypothesis of this study is that due to the zonally-asymmetric driving of the jet, it is affected locally by zonally-dependent processes, thus its variability and response to climate change cannot be fully explained by zonally-symmetric theory. We hypothesize that angular momentum transport driven by localized tropical convection plays a major role in determining the longitudinal structure of the jet, its variability and its response to climate change, particularly in the Southern Hemisphere. Due to the zonally-asymmetric jet structure driven by tropical convection, the momentum budget is affected by processes that are relevant only for a zonally-asymmetric jet: zonal advection, zonal pressure gradients and Rossby wave propagation. The zonally-dependent interaction between the jet and the extratropical eddies reshapes the jet, leading to a zonally-dependent statistically steady state. We hypothesize that all these processes play a role in determining the jet variability and response to climate change.

C.2 Research design and methods

The first two parts of this study will focus on statistical analysis of observational and climate model data. The third part will include controlled experiments using an idealized global circulation model (GCM) to examine the effect of zonally-asymmetric forcing on the jet. We describe in the following paragraphs the statistical methods that will be used, the observational and climate model data that will be analyzed and the idealized model experiment.

C.2.1 Causal detection method

Dynamical atmospheric processes can often be described in a mathematically compact way by defining indices that best capture a specific phenomenon. For example, the Niño-3.4 SST index is a measure for the state of the atmosphere and ocean with respect to El-Niño Southern Oscillation (ENSO). Other important indices include the North Atlantic Oscillation (NAO) index, the Northern Annular mode (NAM) and Southern Annular mode (SAM) indices, the Southern Oscillation Index (SOI) and many more. Many studies define their own indices for targeting specific phenomena. Calculating lagged correlations between different indices assists in identifying processes in the climate system. However, since the correlation between two time series of climatic indices is also affected by processes other than the direct effect of one index on the other, this method might not give the correct indication for the actual dynamical processes. An example relevant for the proposed study is the correlations found between indices of the subtropical and polar-front (eddy-driven) jet position and strength over large longitudinal sectors with the indices of NAO, the Pacific North American (PNA) pattern and Niño 3.4 (Liu et al., 2021). These correlations indicate various potential dynamical connections between tropical and extratropical processes, but the exact causal relation cannot be inferred.

Recent studies have used causal detection methods to quantify the causal connections between climatic variables, described by time series of climatic indices (Kretschmer et al., 2016; Runge et al., 2019; Kretschmer et al., 2021). The method that we plan to use is described in Kretschmer et al. (2016) and Runge et al. (2019).

This method begins with calculating all the relevant time series and the correlations between them. As in the example given below in section C.3.1, if we are interested in the drivers of the Pacific SH winter jet variability, our time series will include the jet strength over this region during the SH winter months, and all other time series we believe could be dynamically connected with this variable, both during and before the winter months. By calculating the correlations between the time series of the Pacific SH winter jet strength index and all other time series we have chosen, we can rule out those that are not statistically significant as being irrelevant. After the identification of the relevant time series, the causal detection algorithm includes two steps:

1. Identifying direct effects between the time series using partial correlations. Variables that are found to be conditionally independent are considered not directly related. This leaves only the potential direct drivers of the variable of interest (which are called "parent processes", Kretschmer et al., 2016).

2. Quantitatively estimating the strength of each causal relation. In this step, a standardized linear regression model is assumed, based on the variable of interest and its parent processes identified in step 1. The coefficients of this model are estimated using an algorithm called "PC algorithm" (named after Peter Spirtes and Clark Glymour, Spirtes et al., 2001).

The outcome of this analysis is a graphical model of the causal effect network describing the connections between all the variables analyzed. Each node in this network describes a variable and the arrows connecting them describe the causal relations between the variables, with the coefficients calculated in step 2 assigned to each respective arrow. The causal effect network can be used to validate or invalidate different hypotheses regarding the causal relations between the variables (Shepherd, 2021).

C.2.2 Observational data

The observational data analysis proposed is described in section C.3.1. The observational data will include ERA5 reanalysis data (Hersbach et al., 2020) for the atmospheric variables such as zonal and meridional wind speeds and temperature. Data of OLR, indicating the strength of tropical convection, will be from the National Oceanic and Atmospheric Administration (NOAA) interpolated OLR data set (Liebmann and Smith, 1996). Sea surface temperature (SST) data will be from the HadISST data set (Rayner et al., 2003).

C.2.3 Comprehensive climate model data

The climate model data analysis proposed is described in section C.3.2. We will use data from the Coupled Model Intercomparison Project Phase 6 (CMIP6). To compare the representation of physical processes in climate models with observational data, we will use data from the historical experiment, which mimics the climate conditions during the time period for which a wide coverage of observational data exists. To investigate how jet driving mechanisms are affected by anthropogenic climate change, we will compare data from the pre-industrial (piControl) experiment with data from the abrupt $4\times CO_2$ experiment. These two experiments include a time period of at least 50 years in which the flow is in statistically steady state, which allows for an examination of the atmospheric circulation maintenance under steady climate conditions.

C.2.4 Idealized model experiment

We plan to use the Model of an idealized Moist Atmosphere (MiMA, Jucker and Gerber, 2017), which is embedded in the modeling framework ISCA (Vallis et al., 2018). This idealized model includes a representation of water vapor and the physical processes of convection, condensation and radiation, including the water vapor radiative effect (as elaborated in Frierson et al., 2006, for an older version of this model). It is considered as an intermediate complexity model (Maher et al., 2019), because its default configuration is an aqua-planet configuration, with no continents, clouds or ice, and it does not include chemical processes. It is more idealized than comprehensive climate models, yet the inclusion of moist processes makes it more complex and more realistic than dry idealized models, such as the Held-Suarez model (Held and Suarez, 1994). This model is able to capture the characteristics of the subtropical and eddy-driven jets (see Figure 4 below), unlike the dry Held-Suarez model, where the circulation tends to be fixed in a merged jet regime, unless it is strongly forced to an empirical jet profile (Wu and Reichler, 2018; White et al., 2024). The model is designed to easily include modifications of the forcing and boundary conditions, and was shown to reproduce a realistic structure of the climatological stationary waves (Garfinkel et al., 2020). We plan to run the model with solstice conditions, to produce both a subtropical and eddy-driven jet, and to add localized tropical diabatic heating, to create a zonally-asymmetric circulation that captures the observed characteristics of the jet (see more details in section C.3.3).

C.3 Work plan and preliminary results

C.3.1 Jet variability drivers in observations

Jet variability at monthly and longer time scales arises from a combination of internal jet-eddies interactions and variability of other atmospheric variables that can be viewed as external to the jet-eddies system. Many studies point to the role of SST variability in the tropics in driving jet variability in both hemispheres (Ding et al., 2012; Li and Wettstein, 2012; Baker et al., 2019; Yang et al., 2020; Gillett et al., 2021; Liu et al., 2021). Zonally-asymmetric tropical convection, induced by zonally-asymmetric SSTs, affects the jet via two main processes: localized angular momentum advection by the upper tropospheric divergent flow (Hoskins and Yang, 2023), and generation of quasi-stationary Rossby waves that propagate from the tropics to the extratropics (Jin and Hoskins, 1995; Inatsu and Hoskins, 2004). While zonal asymmetries arising from topography and land-sea contrast are dominant in the NH, these factors play a secondary role in the jet asymmetry in the SH (Patterson et al., 2020).

To illustrate the importance of zonally-asymmetric tropical convection in driving the zonally-asymmetric jet variability, and to demonstrate the usefulness of causal detection, we present preliminary observational analysis of the SH winter jet. We focus on the Pacific sector, where the jet characteristics are typical of a subtropical jet (see Figure 1), and examine different variables regressed on the jet speed. We chose here to include variables related to tropical convection (measured by OLR), eddy-driven jet strength (measured by the lower tropospheric wind) and the extratropical temperature gradient (measured by the high latitude lower tropospheric tempera-

ture). All of these variables could be connected to processes affecting the Pacific subtropical jet variability.

Figure 2 shows the regression of the upper and lower tropospheric winds, OLR and the lower tropospheric temperature on the jet speed in the Pacific sector during SH winter. A time series is obtained for the jet speed during the winter months (June, July and August), which is denoted by $\overline{u}_{200}^{JJA}$. Similarly, $\overline{u}_{200}^{MJJ}$ and $\overline{u}_{200}^{AMJ}$ denote time series of the jet speed leading by one and two months, respectively, relative to $\overline{u}_{200}^{JJA}$. Time series denoted by $\overline{u}_{850}$, OLR and $\overline{T}_{850}$ represent the lower tropospheric zonal wind, OLR and the lower tropospheric temperature, respectively, averaged over the respective boxes in Fig. 2.

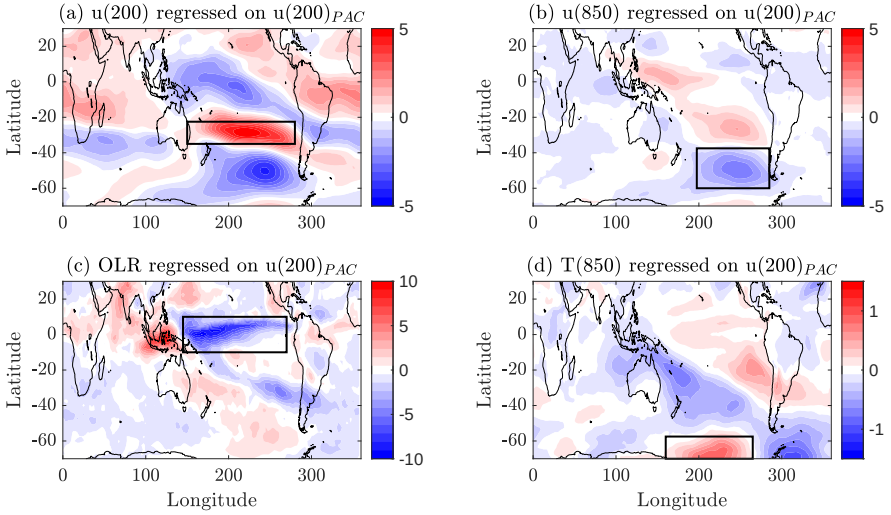

Figure 2: Variables regressed on the upper tropospheric zonal wind in the subtropical Pacific sector (marked by the rectangle box in (a)) during Southern Hemisphere winter (June-August): (a) Upper tropospheric (200 hPa) zonal wind, in m s^{-1}; (b) Lower tropospheric (850 hPa) zonal wind, in m s^{-1}; (c) OLR, in W m^{-2} (negative anomalies indicate stronger convection); (d) Lower tropospheric (850 hPa) temperature in K. The rectangle boxes in each panel indicate the region of averaging to obtain the time series for the causal detection analysis (see text).

Table 1 shows the correlation coefficients between the different time series and $\overline{u}_{200}^{JJA}$. Correlation coefficients with a significance level of 99% and more are shown in bold numbers. Only variables significantly correlated with $\overline{u}_{200}^{JJA}$ at leading months (MMJ and AMJ) are potential drivers of the jet variability on monthly time scales. In this example, four relevant variables are found: $\overline{u}_{200}^{MJJ}$, $\overline{u}_{200}^{AMJ}$, $\overline{u}_{850}^{MJJ}$ and OLR^{MJJ}. The first two are due to the upper tropospheric zonal wind autocorrelation. This leaves tropical convection and eddy-driven jet variability as potential external drivers of the subtropical Pacific jet variability. The high latitude lower tropospheric temperature anomaly is not a potential driver on monthly time scales, though it is correlated with the jet strength during JJA.

The significant correlation does not necessarily imply a causal relation. We next apply the first step in the causal detection method described in section C.2.1, to examine whether the correlation of OLR^{MJJ} with $\overline{u}_{200}^{JJA}$ is an indirect effect, resulting from the synchronous correlation between OLR^{MJJ} and $\overline{u}_{200}^{MJJ}$, combined with the autocorrelation time scale of the jet speed being larger than one month. To test this we calculated the par-

Table 1: Correlation coefficients between the time series of different variables and the upper tropospheric zonal wind in the Pacific sector during June-August. The variables include the upper tropospheric zonal wind ($\overline{u}_{200}$), the lower tropospheric zonal wind ($\overline{u}_{850}$), OLR, and the lower tropospheric temperature ($\overline{T}_{850}$), where each variables is averaged over the respective box in Figure 2. The first row is for the time series during months June-August, i.e. simultaneous with $\overline{u}_{200}^{JJA}$. The second and third rows are for time series during May-July and April-June, respectively, i.e. with a one month and two months lead, respectively, relative to $\overline{u}_{200}^{JJA}$. Correlations marked in bold letters are significant at the 99% level.

	$\overline{u}_{200}$	$\overline{u}_{850}$	OLR	$\overline{T}_{850}$
JJA		**-0.67**	**-0.38**	**0.28**
MJJ	**0.49**	**-0.32**	**-0.36**	0.02
AMJ	**0.36**	-0.23	-0.19	0

tial correlation between OLR^{MJJ} and $\overline{u}_{200}^{JJA}$ conditioned on $\overline{u}_{200}^{MJJ}$. This gives a partial correlation of -0.27 which is significant on a level higher than 99% (see Table 2), supporting the hypothesis that OLR is a direct driver of the jet speed anomaly on a time scale of one month. In contrast, a similar test shows that the lower tropospheric zonal wind is not a direct driver of the jet speed anomaly on a monthly time scale (see Table 2). We also performed a similar test for the Pacific jet during SH summer (December-February). The results (not shown) indicate that OLR is a potential driver of the jet speed anomaly with a lead time of one and two months.

Table 2: As in Table 1, but showing partial correlation coefficients, conditioned on $\overline{u}_{200}^{MJJ}$.

	$\overline{u}_{200}$	$\overline{u}_{850}$	OLR
MJJ		0.06	**-0.27**
AMJ	0.027		

These preliminary results indicate that tropical convection is a direct driver of jet variability in the upper troposphere, while other variables correlated with the jet variability, such as lower tropospheric zonal wind and high latitude lower tropospheric temperature anomalies, are not its direct drivers on monthly time scales. This analysis demonstrates the usefulness of the first step in the causal detection method described in section C.2.1. The second step would be to quantify the strength of each causal connection.

In the proposed research we will include additional time series in the causal detection analysis for the jet variability at each sector and season. The variables for these time series will be chosen so as to represent all plausible influences on the jet variability, based on previous studies and on our observational analysis. We plan to perform the following analysis before applying the causal detection method:

1. Calculating the momentum budget terms and their lagged correlations with respect to jet variability events, defined by anomalies in the local jet strength and latitude over specific longitudinal sectors. This will enables us to evaluate the relative importance of different processes in driving jet variability at each longitudinal sector and season. Comparing the acceleration terms associated with zonally-dependent processes with terms that

affect the zonal-mean momentum budget will enable us to assess the importance of zonal asymmetries for the jet maintenance and variability.

2. Evaluating the relative roles of Rossby wave generation and poleward angular momentum advection in the influence of tropical convection of the jet strength. This can be done by calculating the divergent component of the wind field, from which we can calculate the local Hadley circulation streamfunction (as in Schwendike et al., 2014; Nguyen et al., 2018; Raiter et al., 2024) and the meridional angular momentum advection associated with it. The effect of the Rossby wave source can be calculated using a barotropic model for Rossby wave propagation (Hoskins and Ambrizzi, 1993). We plan to examine to what extent the jet variability over large longitudinal sectors is associated with quasi-stationary Rossby waves excited by a tropical source, and by variations in angular momentum advection by the local Hadley circulation.

The combination of dynamical processes analysis using observational data with causal detection methods will potentially improve our understanding of the mechanisms controlling jet variability over large longitudinal sectors.

C.3.2 Drivers of jet variability and response to climate change in climate models

The robust response of the zonal mean zonal wind to climate change is comprised of a poleward shift of the eddy-driven jet and a strengthening of the subtropical jet. While this zonal-mean response appears in a wide range of climate models under a variety of climate change forcing scenarios and detected in observations, the longitudinally-dependent response is more complex (Barnes and Polvani, 2013; Yang et al., 2020; Waugh et al., 2020). The longitudinal dependance of the jet response is related to the longitudinal dependance of the Hadley cell response. In response to climate change, during SH winter, the meridional circulation weakens over the Indo-Pacific sector and strengthens over the East Pacific (Staten et al., 2019; Raiter et al., 2024). Consistently, the upper-tropospheric subtropical jet slightly weakens and shifts poleward over the Indo-Pacific region and Australia and extends further downstream to the East Pacific (Patterson et al., 2021). The exact mechanisms which drive the local jet response have not yet been elucidated.

The variability between the jet response in different models participating in the CMIP is quite large, compared to the multi-model mean response. It has been recognized in recent years that considering the inter-model variability of the response over specific longitudinal sectors could be useful for identifying model biases and reducing the uncertainty (Oudar et al., 2020; Waugh et al., 2020; Liu et al., 2021; Liu and Grise, 2023; Breul et al., 2023). In particular, Breul et al. (2023) found that inter-model variations in the zonal mean jet latitude during SH winter are a geometric artifact of variations in the eddy-driven Pacific jet strength. This finding helped them explain the relation between the climatological jet latitude and the jet shift in response to climate change found in Simpson and Polvani (2016), which is used as an emergent constraint for the jet shift (Simpson et al., 2021). This striking example demonstrates the importance of examining the jet response over specific longitudinal domains.

We plan to examine the drivers of jet variability in CMIP6 models and to compare them with the observed

drivers found in the first part of the research described in section C.3.1. As a preliminary test, we consider the SH winter jet and its relation with tropical convection in two different climate models. Figure 3 shows the pre-industrial zonal wind and OLR, and their responses to quadrupling CO_2 for two models: CNRM-ESM-1 and MIROC-ES2L. Comparing with Figure 1a,c, we see that the zonal wind in CNRM-ESM-1 is quite realistic, while in MIROC-ES2L the subtropical jet is too strong and extends too far zonally, with weak near-surface winds. The OLR profile is more realistic in MIROC-ES2L, while in CNRM-ESM-1 it is too narrow and concentrated around the equator. The responses of the zonal wind and OLR to quadrupling CO_2 are quite different between the two models. The differences in the zonal wind response might be attributed to the different climatological extratropical circulations (Curtis et al., 2020), or differences in the tropical convection, as indicated by the OLR (Liu and Grise, 2023), or other factors, such as the stratospheric polar vortex (Williams et al., 2024), cloud radiative effects (Voigt and Shaw, 2016), or coupling with the oceanic circulation (Chemke, 2022). In the proposed study we plan to investigate the sources of the inter-model spread in the jet response over different longitudinal sectors.

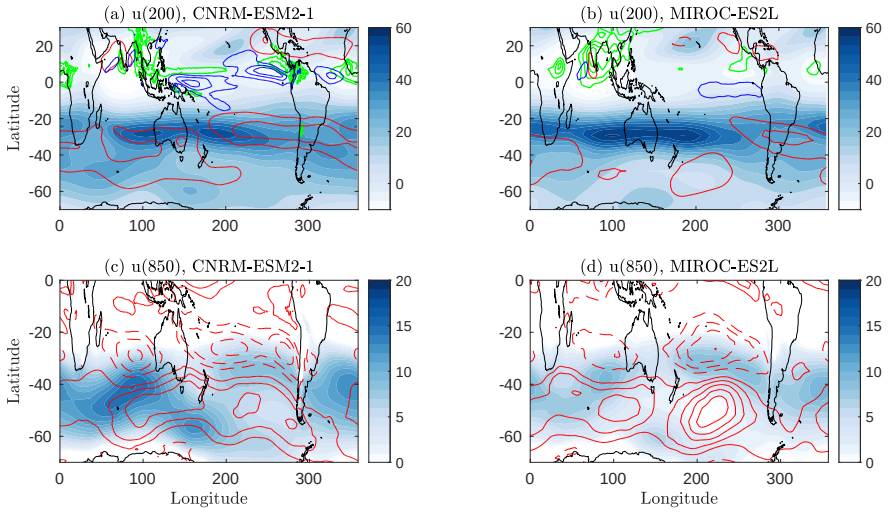

Figure 3: Zonal wind climatology (blue shading, in m s^{-1}), in the upper troposphere (200 hPa) (a,b) and lower troposphere (850 hPa) (c,d), during SH winter, from the pre-industrial simulation of two CMIP6 models: CNRM-ESM-1 (a,c) and MIROC-ES2L (b,d). Red contours show the zonal wind response to quadrupling CO_2, with solid (dashed) contours for positive (negative) values, and a contour interval of 5 m s^{-1} (1 m s^{-1}) for the upper (lower) tropospheric wind response, where the zero contour is omitted. The green and blue contours in (a,b) show the outgoing longwave radiation (OLR), with a contour interval of 10 W m^2, from 180 to 220 W m^2, and its response to quadrupling CO_2, with contour levels -30, -20 and -10 W m^2, indicating increased tropical convection.

In addition to examining the inter-model spread in the jet response, we plan to examine the sources of internal jet variability in the different models. As in the proposed analysis for the observed jet variability, we plan to use causal detection methods to identify drivers of jet variability in CMIP6 models. We take here as an example the pre-industrial simulations of the two models presented in Figure 3. Repeating the same procedure as described in section C.3.1, we calculate the correlations between the winter subtropical jet strength in the

Pacific sector during winter (JJA) and OLR in the tropical Pacific during JJA (simultaneous), MJJ (one month earlier) and AMJ (two months earlier), as well as the lagged autocorrelations of the subtropical jet strength (Table 3). The correlations are higher in MIROC-ES2L than in CNRM-ESM-1, for both the autocorrelation of the subtropical jet strength and for its correlation with OLR (left half of Table 3).

Table 3: Correlation coefficients (left half of the table) between the time series of the Pacific subtropical jet strength during JJA ($\overline{u}_{200}^{JJA}$) and both the subtropical jet strength one (MJJ) or two (AMJ) months earlier and the outgoing longwave radiation (OLR) during JJA, MJJ and AMJ. The correlations are calculated for the internal monthly variability in two CMIP6 models: CNRM-ESM-1 and MIROC-ES2L. The right half of the table shows the relevant partial correlations with $\overline{u}_{200}^{JJA}$, after conditioning for the subtropical jet strength during MJJ ($\overline{u}_{200}^{MJJ}$). Correlations marked in bold letters are significant at the 99% level.

	Correlation with $\overline{u}_{200}^{JJA}$				Conditioned on $\overline{u}_{200}^{MJJ}$			
	CNRM-ESM-1		MIROC-ES2L		CNRM-ESM-1		MIROC-ES2L	
	$\overline{u}_{200}$	OLR	$\overline{u}_{200}$	OLR	$\overline{u}_{200}$	OLR	$\overline{u}_{200}$	OLR
JJA		**-0.31**		**-0.55**				
MJJ	**0.49**	**-0.48**	**0.65**	**-0.67**		**-0.30**		**-0.47**
AMJ	**0.36**	**-0.49**	**0.52**	**-0.39**	-0.03	**-0.24**	-0.11	**-0.29**

Conditioning for the subtropical jet strength during MJJ reduces the correlations, but the correlations between the jet strength and OLR one and two months earlier remain significant (right half of Table 3), indicating that the high correlations partly represent an indirect connection, mediated by the subtropical jet strength during MJJ, and are partly due to a direct driving of the jet variability by tropical convection. The direct driving of the jet variability by tropical convection is high in MIROC-ES2L compared to CNRM-ESM-1 and to the observed values (see Table 2). To get a more accurate and wide view of causal drivers of the subtropical jet variability in models, more relevant variables need to be added to the analysis, and the subsequent steps in the causal detection analysis should be applied, as described in section C.2.1.

We propose to extend this analysis to all the CMIP6 models for which the relevant data is available. The outcome will help evaluate the extent to which different models capture the processes driving the jet variability. This could enable an improved evaluation of model performance and thus a decrease in the uncertainty of projections regarding the response of the jet and its variability properties to climate change.

C.3.3 Jet variability in an idealized model with localized tropical heating

A direct way to examine causal relations in the atmospheric circulation is to use a numerical model, where it is possible to actively control certain processes. The idealized model (MiMA, described in section C.2.4) will be used to examine the jet dynamics in the presence of a zonally-asymmetric tropical heat source. Because the model includes moist processes, it is able to qualitatively capture the sporadic localized nature of tropical convection (Frierson et al., 2006; Frierson, 2007), which is an essential factor for creating a realistic subtropical jet (Hoskins and Yang, 2023). Localized tropical heating added to a dry model produces a transient subtropical jet, which is not maintained in steady state (Williams et al., 2007). In fact, a realistic-looking subtropical jet is

rarely produced using a dry model, except when the model is forced using observational data (Kim and Lee, 2004; Wu and Reichler, 2018). The preliminary results presented here show that MiMA is able to capture the localized structure of the subtropical jet, driven by localized tropical heating, as seen in observations.

We performed a preliminary simulation of NH winter conditions, created by using a solar insolation profile and a prescribed sea surface temperature profile that peak in the Southern Hemisphere tropics. A localized diabatic heat source was added around the latitude of maximum ascent, with a limited longitudinal extent. The localized heat source drives a localized jet which resembles the observed subtropical jet, while an eddy-driven jet exists at other longitudes (Figure 4, compare with Figure 1). This preliminary result demonstrates that the idealized model is suitable for studying the response of the jet to a localized tropical heating.

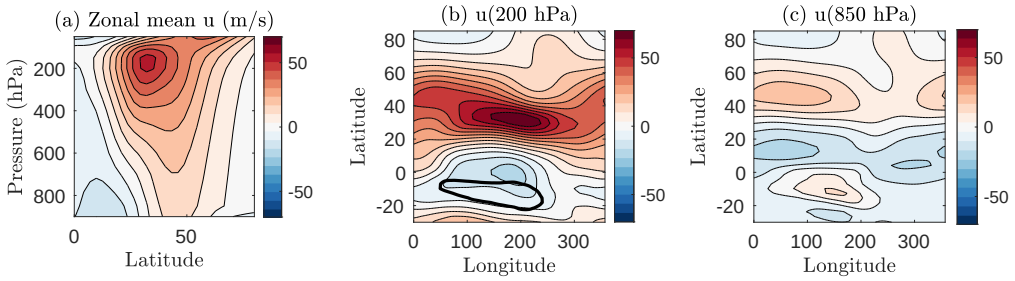

Figure 4: Zonal wind (in m s^{-1}) in the idealized model simulation with additional localized tropical heating, averaged over the statistically steady state period. (a) Zonal mean zonal wind as a function of latitude and pressure. (b) Zonal wind at pressure level 200 hPa, as a function of longitude and latitude. (c) as in (b) but for the pressure level 850 hPa. The thick black contour in (b) marks the 2 K day^{-1} diabatic heating contour at pressure level 300 hPa. The region inside this contour has larger values of diabatic heating.

Using this model, we will perform a series of simulations in which we will vary several properties of the tropical heat source across a wide range of values and examine their effect on the jet climatological profile and variability. The controlled properties of the heat source will include its longitudinal, latitudinal and vertical extent, its distance from the equator and its strength. This parameter sweep will allow us to produce a wide range of jet profiles, with varying dominance of the subtropical jet or eddy-driven jet over a wide range of longitudinal extents. Once the desired range of circulations is achieved, we will analyze the jet driving mechanisms in each simulation. The simulations will include steady state simulations and ensembles of switch-on simulations in which the localized tropical heating is abruptly changed, which allows for an analysis of the transition between steady states.

The analysis of the jet driving mechanisms will include the following aspects: (1) The zonal momentum budget as a function of longitude and latitude in the upper troposphere. Each of the terms in the momentum budget will be calculated for the steady state and for the transition periods, to identify processes leading to changes in the jet properties. (2) Lagged regressions of different variables with respect to events of extreme jet properties. This includes, for example, an analysis of the meridional streamfunction and eddy heat and momentum fluxes around events of strong jet. (3) Analysis of Rossby wave propagation, in order to determine its role in shaping the zonally asymmetric jet structure. (4) Causal detection of jet variability drivers in the

model, for comparison with the results of the observational data analysis.

We expect the results from the idealized model simulations will provide an overview of the dynamics leading to the zonally asymmetric jet structure arising from asymmetric tropical heating. In particular, it will reveal the processes leading to the zonal transition in the jet characteristics between the subtropical and eddy-driven type of jets. It was suggested by Williams et al. (2007) that the zonal structure of the springtime SH jet arises from the following process: Localized tropical heating drives a localized subtropical jet, which is baroclinically unstable and leads to growth of midlatitude eddies on its downstream side, which in turn drive an eddy-driven jet further downstream. They used a dry model to test this hypothesis, but the dry model was only able to reproduce a realistic zonal structure of the jet for a limited period of time. As demonstrated by our preliminary results, the moist model we plan to use is able to reproduce this realistic structure in statistically steady state, and therefore it is more suitable for examining the processes leading to the zonally asymmetric jet structure.

C.4 The researcher's resources for conducting the research

The PI is a faculty member in the Department of Natural Sciences at the Open University of Israel. She has published many papers on various aspects of the midlatitude atmospheric circulation and jet stream dynamics. The Open University of Israel owns a high performance computing (HPC) system, with sufficient cores for running the idealized model MiMA at T85 resolution, which is sufficient for capturing the dynamics relevant for this work. The university employs a full-time technical support team for the HPC system. On this system, 320 cores and 50TB of storage are dedicated exclusively to the PI's group. This group has already published several papers based on results from running MiMA and observational and climate model data analysis using this HPC system (Lachmy and Kaspi, 2020; Lachmy, 2022; Peles and Lachmy, 2023; Ghosh et al., 2024). In this proposal, we are asking for funding to extend the storage capacity by another 50TB, to store more reanalysis (observational) data and climate model data output on the HPC system. This is needed since most of the data we stored so far was zonally averaged (i.e., data as a function of latitude, pressure and time), whereas in the proposed research we will need to save longitudinally-dependent data (as a function of longitude, latitude and time) on several pressure levels.

The data analysis methods which we are suggesting to use are mostly similar to methods we used in the previous research, except for the causal detection analysis. For this purpose we plan to collaborate with Prof. Marlene Kretschmer from Leipzig University, who kindly shared her causal detection code (see Kretschmer et al., 2016), as indicated in her letter attached to this proposal.

C.5 Expected results and pitfalls

We expect the proposed research will advance the understanding of jet dynamics under zonally asymmetric conditions. The observational data analysis is expected to confirm or negate various hypotheses for the processes that control the jet dynamics at specific longitudinal sectors and seasons (e.g., Nakamura et al., 2004; Williams et al., 2007; Hoskins and Yang, 2023). Previous studies examined correlations between jet variability

and different climatic variables, such as eddy momentum flux and OLR. While this type of analysis indicates consistency or inconsistency of the data with different hypotheses, it suffers from ambiguity, since correlations are not necessarily due to causal relations. We expect that using the causal detection analysis will reveal which of these correlations are due to causal relations, at what time scales and to what extent. We acknowledge that causal detection has its limitations. This method assumes that all relevant processes are included in the analysis, which might not be the case, therefore the relations detected should be considered as potential causal relations (Barnes et al., 2019). Other underlying assumptions include stationarity and Gaussian distributions of the model variables, as well as linear relations between the variables. The results could be sensitive to the choice of time scale for the time series. We will perform the necessary sensitivity tests to determine the optimal choice of variables and time scales needed to capture the causal relations in the most reliable possible way. Causal detection relies on previous knowledge of the potential relevant variables affecting the variable of interest. We therefore include in the observational data analysis calculations of momentum budget terms and Rossby wave propagation, to obtain a more knowledgable picture of the processes controlling the jet variability at large longitudinal sectors, before performing the Causal detection analysis.

The climate model data analysis is expected to add insight to the inter-model jet variability sources. We expect that by revealing the different associations between jet properties and their driving processes in models we will be able to point toward specific processes that need to be captured more realistically in order to simulate the jet dynamics correctly. This could help assess which models are expected to produce a more reliable projection for the jet response to climate change, for example by identifying emergent constraints related to jet driving mechanisms (Simpson et al., 2021). In addition to inter-model variability, the analysis could detect sources for biases in the jet representation across all models. While CMIP6 models are improved compared to CMIP5, there are still biases in the jet representation (Bracegirdle et al., 2020). By comparing the jet driving processes in models to those in observations we expect to shed light on the sources of these biases.

The idealized model simulations are expected to yield new information about the response of the jet to localized tropical heating, which has not yet been studied in a moist model. We expect that this would advance our understanding of the processes determining the jet properties and their longitudinal transitions seen in observations. The dynamics of the jet in the real atmosphere are affected also by processes not included in the model, such as ocean variability, cloud radiative effect and sea ice processes. However, since tropical convection was found to play a major role in the longitudinal structure of the jet, we expect that these simulations will capture an important aspect of the dynamics. The comparison between the model simulations and the observational analysis will reveal the extent to which the model captures the actual dynamics.

References

[1] H. S. Baker, T. Woollings, C. E. Forest, and M. R. Allen. The linear sensitivity of the North Atlantic Oscillation and eddy-driven jet to SSTs. *J. Climate*, 32:6491–6511, 2019.

[2] E. A. Barnes and L. Polvani. Response of the midlatitude jets, and of their variability, to increased greenhouse gases in the CMIP5 models. *J. Climate*, 26:7117–7135, 2013.

[3] E. A. Barnes, S. M. Samarasinghe, I. Ebert-Uphoff, and J. C. Furtado. Tropospheric and stratospheric causal pathways between the MJO and NAO. *J. Geophys. Res. -Atmos.*, 124:9356–9371, 2019.

[4] T. J. Bracegirdle, C. R. Holmes, J. S. Hosking, G. J. Marshall, M. Osman, M. Patterson, and T. Rackow. Improvements in circumpolar Southern Hemisphere extratropical atmospheric circulation in CMIP6 compared to CMIP5. *Earth and Space Science*, 7:e2019EA001065, 2020.

[5] P. Breul, P. Ceppi, and T. G. Shepherd. Revisiting the wintertime emergent constraint of the Southern Hemispheric midlatitude jet response to global warming. *Wea. Climate Dyn.*, 4:39–47, 2023.

[6] R. Chemke. The future poleward shift of Southern Hemisphere summer mid-latitude storm tracks stems from ocean coupling. *Nat. Commun.*, 13:1730, 2022.

[7] P. E. Curtis, P. Ceppi, and G. Zappa. Role of the mean state for the Southern Hemispheric jet stream response to CO_2 forcing in CMIP6 models. *Environmental Research Letters*, 15:064011, 2020.

[8] Q. Ding, E. J. Steig, D. S. Battisti, and J. M. Wallace. Influence of the tropics on the Southern Annular Mode. *J. Climate*, 25(18):6330–6348, 2012.

[9] D. M. W. Frierson. The dynamics of idealized convection schemes and their effect on the zonally averaged tropical circulation. *J. Atmos. Sci.*, 64:1959–1976, 2007.

[10] D. M. W. Frierson, I. M. Held, and P. Zurita-Gotor. A gray-radiation aquaplanet moist GCM. Part I: Static stability and eddy scale. *J. Atmos. Sci.*, 63:2548–2566, 2006.

[11] C. I. Garfinkel, I. White, E. P. Gerber, M. Jucker, and M. Erez. The building blocks of Northern Hemisphere wintertime stationary waves. *J. Climate*, 33:5611–5633, 2020.

[12] S. Ghosh, O. Lachmy, and Y. Kaspi. The role of diabatic heating in the midlatitude atmospheric circulation response to climate change. *J. Climate*, 37:2987–3009, 2024.

[13] Z. E. Gillett, H. H. Hendon, J. M. Arblaster, and E.-P. Lim. Tropical and extratropical influences on the variability of the Southern Hemisphere wintertime subtropical jet. *J. Climate*, 34:4009–4022, 2021.

[14] I. M. Held and A. Y. Hou. Nonlinear axially symmetric circulations in a nearly inviscid atmosphere. *J. Atmos. Sci.*, 37:515–533, 1980.

[15] I. M. Held and M. J. Suarez. A proposal for the intercomparison of the dynamical cores of atmospheric general circulation models. *Bull. Amer. Meteor. Soc.*, 75(10):1825–1830, 1994.

[16] H. Hersbach, B. Bell, P. Berrisford, S. Hirahara, A. Horányi, J. Muñoz-Sabater, J. Nicolas, C. Peubey, R. Radu, D. Schepers, et al. The ERA5 global reanalysis. *Quart. J. Roy. Meteor. Soc.*, 146:1999–2049, 2020.

[17] B. J. Hoskins and T. Ambrizzi. Rossby wave propagation on a realistic longitudinally varying flow. *J. Atmos. Sci.*, 50(12):1661–1671, 1993.

[18] B. J. Hoskins and G-Y. Yang. The detailed dynamics of the Hadley cell. Part II: December–February. *J. Climate*, 34(2):805–823, 2021.

[19] B. J. Hoskins and G-Y. Yang. A global perspective on the upper branch of the Hadley Cell. *J. Climate*, 36:6749–6762, 2023.

[20] B. J. Hoskins, G.-Y. Yang, and R. M. Fonseca. The detailed dynamics of the June–August Hadley cell. *Quart. J. Roy. Meteor. Soc.*, 146(727):557–575, 2020.

[21] M. Inatsu and B. J. Hoskins. The zonal asymmetry of the Southern Hemisphere winter storm track. *J. Climate*, 17:4882–4892, 2004.

[22] F. Jin and B. J. Hoskins. The direct response to tropical heating in a baroclinic atmosphere. *J. Atmos. Sci.*, 52:307–319, 1995.

[23] M. Jucker and E. P. Gerber. Untangling the annual cycle of the tropical tropopause layer with an idealized moist model. *J. Climate*, 30:7339–7358, 2017.

[24] H. K. Kim and S. Lee. The wave - zonal mean flow interaction in the southern hemisphere. *J. Atmos. Sci.*, 61:1055–1067, 2004.

[25] M. Kretschmer, D. Coumou, J. F. Donges, and J. Runge. Using causal effect networks to analyze different Arctic drivers of midlatitude winter circulation. *J. Climate*, 29:4069–4081, 2016.

[26] M. Kretschmer, S. V. Adams, A. Arribas, R. Prudden, N. Robinson, E. Saggioro, and T. G. Shepherd. Quantifying causal pathways of teleconnections. *Bull. Amer. Meteor. Soc.*, 102:E2247–E2263, 2021.

[27] O. Lachmy. The relation between the latitudinal shifts of midlatitude diabatic heating, eddy heat flux, and the eddy-driven jet in CMIP6 models. *J. Geophys. Res. -Atmos.*, 127:e2022JD036556, 2022.

[28] O. Lachmy and N. Harnik. The transition to a subtropical jet regime and its maintenance. *J. Atmos. Sci.*, 71:1389–1409, 2014.

[29] O. Lachmy and N. Harnik. Wave and jet maintenance in different flow regimes. *J. Atmos. Sci.*, 73: 2465–2484, 2016.

[30] O. Lachmy and Y. Kaspi. The role of diabatic heating in Ferrel cell dynamics. *Geophys. Res. Lett.*, 47: e2020GL090619, 2020.

[31] S. Lee and H. K. Kim. The dynamical relationship between subtropical and eddy-driven jets. *J. Atmos. Sci.*, 60:1490–1503, 2003.

[32] C. Li and J. J. Wettstein. Thermally driven and eddy-driven jet variability in reanalysis. *J. Climate*, 25: 1587–1596, 2012.

[33] B. Liebmann and C. A. Smith. Description of a complete (interpolated) outgoing longwave radiation dataset. *Bull. Amer. Meteor. Soc.*, 77:1275–1277, 1996.

[34] X. Liu and K. M. Grise. Implications of warm pool bias in CMIP6 models on the Northern Hemisphere wintertime subtropical jet and precipitation. *Geophys. Res. Lett.*, 50:e2023GL104896, 2023.

[35] X. Liu, K. M. Grise, D. F. Schmidt, and R. E. Davis. Regional characteristics of variability in the Northern Hemisphere wintertime polar front jet and subtropical jet in observations and CMIP6 models. *J. Geophys. Res. -Atmos.*, 126:e2021JD034876, 2021.

[36] D. J. Lorenz and D. L. Hartmann. Eddy–zonal flow feedback in the Southern Hemisphere. *J. Atmos. Sci.*, 58:3312–3327, 2001.

[37] D. J. Lorenz and D. L. Hartmann. Eddy–zonal flow feedback in the Northern Hemisphere winter. *J. Climate*, 16:1212–1227, 2003.

[38] P. Maher, E. P. Gerber, B. Medeiros, T. M. Merlis, S. Sherwood, A. Sheshadri, A. H. Sobel, G. K. Vallis, A. Voigt, and P. Zurita-Gotor. Model hierarchies for understanding atmospheric circulation. *Reviews of Geophysics*, 57(2):250–280, 2019.

[39] H. Nakamura and A. Shimpo. Seasonal variations in the Southern Hemisphere storm tracks and jet streams as revealed in a reanalysis dataset. *J. Climate*, 17:1828–1844, 2004.

[40] H. Nakamura, T. Sampe, Y. Tanimoto, and A. Shimpo. Observed associations among storm tracks, jet streams and midlatitude oceanic fronts. *Earth's Climate: The Ocean–Atmosphere Interaction, Geophys. Monogr*, 147:329–345, 2004.

[41] H. Nguyen, H. H. Hendon, E-P. Lim, G. Boschat, E. Maloney, and B. Timbal. Variability of the extent of the Hadley circulation in the Southern Hemisphere: A regional perspective. *Clim. Dyn.*, 50:129–142, 2018.

[42] T. Oudar, J. Cattiaux, and H. Douville. Drivers of the northern extratropical eddy-driven jet change in CMIP5 and CMIP6 models. *Geophys. Res. Lett.*, 47:e2019GL086695, 2020.

[43] M. Patterson, T. Woollings, T. J. Bracegirdle, and N. T. Lewis. Wintertime Southern Hemisphere jet streams shaped by interaction of transient eddies with Antarctic orography. *J. Climate*, 33:10505–10522, 2020.

[44] M. Patterson, T. Woollings, and T. J. Bracegirdle. Tropical and subtropical forcing of future Southern Hemisphere stationary wave changes. *J. Climate*, 34:7897–7912, 2021.

[45] O. Peles and O. Lachmy. Estimating the lowest latitude of baroclinic growth. *J. Atmos. Sci.*, 80:1401–1414, 2023.

[46] D. Raiter, E. Galanti, R. Chemke, and Y. Kaspi. Linking future tropical precipitation changes to zonally-asymmetric large-scale meridional circulation. *Geophys. Res. Lett.*, 51:e2023GL106072, 2024.

[47] N. A. A. Rayner, D. E. Parker, E. B. Horton, C. K. Folland, L. V. Alexander, D. P. Rowell, E. C. Kent, and A. Kaplan. Global analyses of sea surface temperature, sea ice, and night marine air temperature since the late nineteenth century. *J. Geophys. Res. -Atmos.*, 108:4407, 2003.

[48] J. Runge, V. Petoukhov, and J. Kurths. Quantifying the strength and delay of climatic interactions: The ambiguities of cross correlation and a novel measure based on graphical models. *J. Climate*, 27:720–739, 2014.

[49] J. Runge, S. Bathiany, E. Bollt, G. Camps-Valls, D. Coumou, E. Deyle, C. Glymour, M. Kretschmer, M. D. Mahecha, J. Muñoz-Marí, et al. Inferring causation from time series in Earth system sciences. *Nat. Commun.*, 10:2553, 2019.

[50] J. Schwendike, P. Govekar, M. J. Reeder, R. Wardle, G. J. Berry, and C. Jakob. Local partitioning of the overturning circulation in the tropics and the connection to the Hadley and Walker circulations. *J. Geophys. Res. -Atmos.*, 119:1322–1339, 2014.

[51] T. A Shaw. Mechanisms of future predicted changes in the zonal mean mid-latitude circulation. *Current Climate Change Reports*, 5(4):345–357, 2019.

[52] T. G. Shepherd. Bringing physical reasoning into statistical practice in climate-change science. *Climatic Change*, 169:2, 2021.

[53] I. R. Simpson and L. M. Polvani. Revisiting the relationship between jet position, forced response, and annular mode variability in the southern midlatitudes. *Geophys. Res. Lett.*, 43(6):2896–2903, 2016.

[54] I. R. Simpson, K. A. McKinnon, F. V. Davenport, M. Tingley, F. Lehner, A. Al Fahad, and D. Chen. Emergent constraints on the large-scale atmospheric circulation and regional hydroclimate: Do they still work in CMIP6 and how much can they actually constrain the future? *J. Climate*, 34:6355–6377, 2021.

[55] C. Spensberger, C. Li, and T. Spengler. Linking instantaneous and climatological perspectives on eddy-driven and subtropical jets. *J. Climate*, 36:8525–8537, 2023.

[56] P. Spirtes, C. Glymour, and R. Scheines. *Causation, prediction, and search*. Bradford, 2001.

[57] P. W. Staten, K. M. Grise, S. M. Davis, K. Karnauskas, and N. Davis. Regional widening of tropical overturning: Forced change, natural variability, and recent trends. *J. Geophys. Res. -Atmos.*, 124:6104–6119, 2019.

[58] G. K. Vallis, G. Colyer, R. Geen, E. Gerber, M. Jucker, P. Maher, A. Paterson, M. Pietschnig, J. Penn, and S. I. Thomson. Isca, v1. 0: A framework for the global modelling of the atmospheres of Earth and other planets at varying levels of complexity. *Geosci. Model Dev.*, 11:843–859, 2018.

[59] A. Voigt and T. A. Shaw. Impact of regional atmospheric cloud radiative changes on shifts of the extratropical jet stream in response to global warming. *J. Climate*, 29:8399–8421, 2016.

[60] D. W. Waugh, K. M. Grise, W. J. M. Seviour, S. M. Davis, N. Davis, O. Adam, S.-W. Son, I. R. Simpson, P. W. Staten, A. C. Maycock, C. C. Ummenhofer, T. Birner, and A. Ming. Revisiting the relationship among metrics of tropical expansion. *J. Climate*, 31:7565–7581, 2018.

[61] D. W. Waugh, A. Banerjee, J. C. Fyfe, and L. M. Polvani. Contrasting recent trends in Southern Hemisphere westerlies across different ocean basins. *Geophys. Res. Lett.*, 47:e2020GL088890, 2020.

[62] I. P. White, O. Lachmy, and N. Harnik. Influence of diabatic heating on the maintenance of the midlatitude jet. *Quart. J. Roy. Meteor. Soc.*, 2024.

[63] L. N. Williams, S. Lee, and S. W. Son. Dynamics of the southern hemisphere spiral jet. *J. Atmos. Sci.*, 64: 548–563, 2007.

[64] R. S. Williams, G. J. Marshall, X. Levine, L. S. Graff, D. Handorf, N. M. Johnston, A. Y. Karpechko, A. Orr, W. J. Van de Berg, R. R. Wijngaard, et al. Future antarctic climate: Storylines of midlatitude jet strengthening and shift emergent from cmip6. *J. Climate*, 37:2157–2178, 2024.

[65] T. Woollings, M. Drouard, C. H. O'Reilly, D. M. H. Sexton, and C. McSweeney. Trends in the atmospheric jet streams are emerging in observations and could be linked to tropical warming. *Commun. Earth Environ.*, 4:125, 2023.

[66] Z. Wu and T. Reichler. Towards a more earth-like circulation in idealized models. *J. Adv. Model. Earth Syst.*, 10(7):1458–1469, 2018.

[67] D. Yang, J. M. Arblaster, G. A. Meehl, M. H. England, E.-P. Lim, S. Bates, and N. Rosenbloom. Role of tropical variability in driving decadal shifts in the Southern Hemisphere summertime eddy-driven jet. *J. Climate*, 33:5445–5463, 2020.